Exploration of Foods and Foodomics

Open Exploration

Open Access Original Article

Electrochemical sensing of nitrite in drinking water using multi-walled carbon nanotubes modified platinum electrode

Merzak Doulache[1*], Nurgul K. Bakirhan[2*], Boubakeur Saidat[1], Mohamed Trari[3], Sibel A. Ozkan[4]

[1]Laboratory of Physical Chemistry of Materials (LPCM), Faculty of Sciences, (UATL) BP 37G, Laghouat 03000, Algeria
[2]Department of Analytical Chemistry, Gulhane Faculty of Pharmacy, University of Health Sciences, Ankara 06018, Türkiye
[3]Laboratory of Storage and Valorization of Renewable Energies (LSVRE), Faculty of Chemistry (USTHB), BP 32, Algiers 16111, Algeria
[4]Department of Analytical Chemistry, Faculty of Pharmacy, Ankara University, Ankara 06560, Türkiye

***Correspondence:** Merzak Doulache, Laboratory of Physical Chemistry of Materials (LPCM), Faculty of Sciences, (UATL) BP 37G, Laghouat 03000, Algeria. m.doulache@lagh-univ.dz; doulache@yahoo.fr | Nurgul K. Bakirhan, Department of Analytical Chemistry, Gulhane Faculty of Pharmacy, University of Health Sciences, Ankara 06018, Türkiye. nurgulk44@gmail.com
Academic Editor: Zhaowei Zhang, Chinese Academy of Agricultural Sciences, China
Received: June 9, 2024 **Accepted:** August 15, 2024 **Published:** November 18, 2024

Cite this article: Doulache M, Bakirhan NK, Saidat B, Trari M, Ozkan SA. Electrochemical sensing of nitrite in drinking water using multi-walled carbon nanotubes modified platinum electrode. Explor Foods Foodomics. 2024;2:659–71. https://doi.org/10.37349/eff.2024.00057

Abstract

Aim: The scope of the present study was to elaborate a nitrite electrochemical sensor using multi-walled carbon nanotubes (MWCNTs) modified Pt electrode.

Methods: The electrocatalytic activity of the proposed sensor was studied by cyclic voltammetry (CV), chronoamperometry (ChAm), and electrochemical impedance spectroscopy (EIS). Then electrochemical detection of nitrite was performed using square wave voltammetry (SWV).

Results: The MWCNTs/Pt electrode exhibits good electrocatalytic activity for the oxidation of nitrite in neutral pH. Subsequently, the fabricated electrochemical sensor shows a high sensitivity for the NO_2^- determination and a low limit of detection (LOD) (0.1 µM) in a wide linear concentration range (1.0–1,000 µM).

Conclusions: This electrochemical sensor has cost-effective, anti-interference capability as well as good stability, reproducibility, and applicability.

Keywords

Multi-walled carbon nanotubes, modified electrode, nitrite ion, electrochemical sensor

Introduction

Nitrite is widely present in daily life and the natural environment, but its overuse and potential toxicity is a serious health threat. It reacts with the blood pigments to form meta-hemoglobin, resulting in oxygen depletion in the tissue and the excess quantity in the blood produces an irreversible oxidation of the

hemoglobin [1]. Moreover, the gastric reaction of NO_2^- with amines and amides generates *N*-nitrosamine compounds, suspected to be carcinogens [2]. According to World Health Organization (WHO) standards, the maximum allowable content of NO_2^- in drinking water is 43.48 μM [3]. Therefore, it is imperative to develop sensitive strategies for the detection of NO_2^- in drinking water and food. In this respect, certain techniques such as spectrophotometry [4], chromatography [5], polarography [6], electrophoresis [7], and flow injection analysis [8] were used for this purpose. Nevertheless, it should be emphasized that these methods involve long analysis times, energy costs, and complicated procedures. Among the suggested techniques, electrochemistry remains an efficient alternative owing to its simplicity and fast response to the operation modes [9–12]. However, it is still a challenge to improve the sensitivity and other properties of the electrochemical nitrite sensors.

In order to improve the electrochemical sensing properties, great efforts have been focused on electrochemical sensors by modifying the electrode with electron transfer mediators. In the last few years, multi-walled carbon nanotubes (MWCNTs) have attracted enormous interest because of their unique structural, mechanical, and electronic properties. Some of these properties include high chemical and thermal stability, high elasticity, high tensile strength, and in some instances, metallic conductivity [13, 14]. The modification of electrode substrates with MWCNT for use in analytical sensing is well documented to result in low limit of detections (LODs), increased sensitivities, reduced overpotentials, and resistance to surface fouling [15, 16]. The best solvents reported for effecting CNT dispersions are *N*,*N*-dimethylformamide (DMF) and *N*-methylpyrrolidone [17]. Further, several strategies were used to build CNT thin films by the layer-by-layer method and the dispersion without chemical functionalization of CNTs on the electrode surface [18, 19].

In the current work, we propose a sensitive and low-cost technique for the analysis of NO_2^- in an aqueous environment using MWCNTs coated Pt electrode. The proposed sensor was characterized by cyclic voltammetry (CV), electrochemical impedance spectroscopy (EIS), and chronoamperometry (ChAm) methods. The oxidation of nitrite ion was investigated with square wave voltammetry (SWV). In particular, the oxidation of nitrite was found at less positive potentials proving the catalytical effect of MWCNTs/Pt electrode. The effect of possible interferents was examined using 100-fold concentrated solutions of mineral and organic substances. The analytical applicability of the electrode was demonstrated in mineral and source water samples with a high reliability. To the best of our knowledge, this is the first time we have determined nitrite ion using MWCNTs coated Pt electrode. Such an electrode system provided a non-enzymatic sensing platform with good electrocatalytic properties and sensitivity for nitrite detection, a fast response time, and low-cost analysis.

Materials and methods

Reagents and materials

MWCNTs were supplied from DropSens, $HCON(CH_3)_2$ (68%, Sigma-Aldrich), and $NaNO_2$ (98%, Fluka) were of analytical quality. The phosphate-buffered solution (PBS) was elaborated by mixing 0.1 M NaH_2PO_4 and Na_2HPO_4 solutions (98%, Sigma-Aldrich). Deionized water was employed for all preparations.

The electrochemical study was carried out at room temperature in a three-electrode arrangement in the standard cell; the data were collected with a potentiostat/galvanostat (model PGZ402, Radiometer Analytical, France) coupled with a PC-computer. A saturated calomel electrode (SCE) (Hg/Hg_2Cl_2) as a reference, Pt wire as an auxiliary electrode, and MWCNTs/Pt as a working electrode (Ø = 2 mm) were used on the electrochemical cell. The pH was measured with a digital pH meter (model inoLab® pH 7110).

Preparation of modified electrode

The working electrode was mechanically polished to a mirror-like surface with Al_2O_3 (0.3 μm) slurry on a polishing cloth. After being washed with distilled water, the bare electrode was sonicated (5 min) in ethanol and dried at ambient temperature. A suspension was prepared by dispersing 1 mg MWCNTs in 1 mL DMF under sonication for 30 min. The MWCNT-modified Pt was prepared by casting a known volume (3 μL) of the mentioned suspension on the Pt electrode surface using a micropipette and left to dry at room

temperature. The surface was electrochemically cleaned in supporting electrolyte by CV between –0.25 V and 1.5 V for several cycles after each run to remove the adsorbed substances. Then the electrode surface was rinsed with distilled water.

Analytical procedure

MWCNTs/GCE (glassy carbon electrode) was electrochemically activated in PBS solution (0.1 M, pH 7.0) under scanning potential between –0.25 and 1.2 V at 50 mVs^{-1} until a reproducible cyclic voltammogram was obtained. The sensor was transferred into a 10 mL glass standard cell filled with PBS solution, and aliquots of the stock solution were added. The calibration graph was constructed from the SW voltammograms plotted by successive additions from aliquots of the stock solution to 10 mL of PBS solution (0.1 M, pH 7.0); each concentration was measured in triplicate. All potential were referred to the SCE at an ambient temperature.

Results

Electrooxidation of nitrite on MWCNTs/Pt electrode

Figure 1a illustrates the voltammograms of the bare electrode and MWCNTs/Pt in 0.1 M PBS (pH 7.0) in the absence and the presence of 1.0 mM NO_2^- at a scan rate of 50 mVs^{-1}. As expected, no signal could appear on the bare Pt and modified electrode in pure 0.1 M PBS at pH 7.0. However, in the addition of 1.0 mM NO_2^-, an oxidation peak appears at 0.70 V and no reduction peak appears in the reversal scan. The cyclic voltammogram of 1.0 mM NO_2^- at the bare Pt under identical conditions is given for comparison. As shown, the oxidation peak is obtained at about 0.77 V, and no reduction peak appears in the reversal scan.

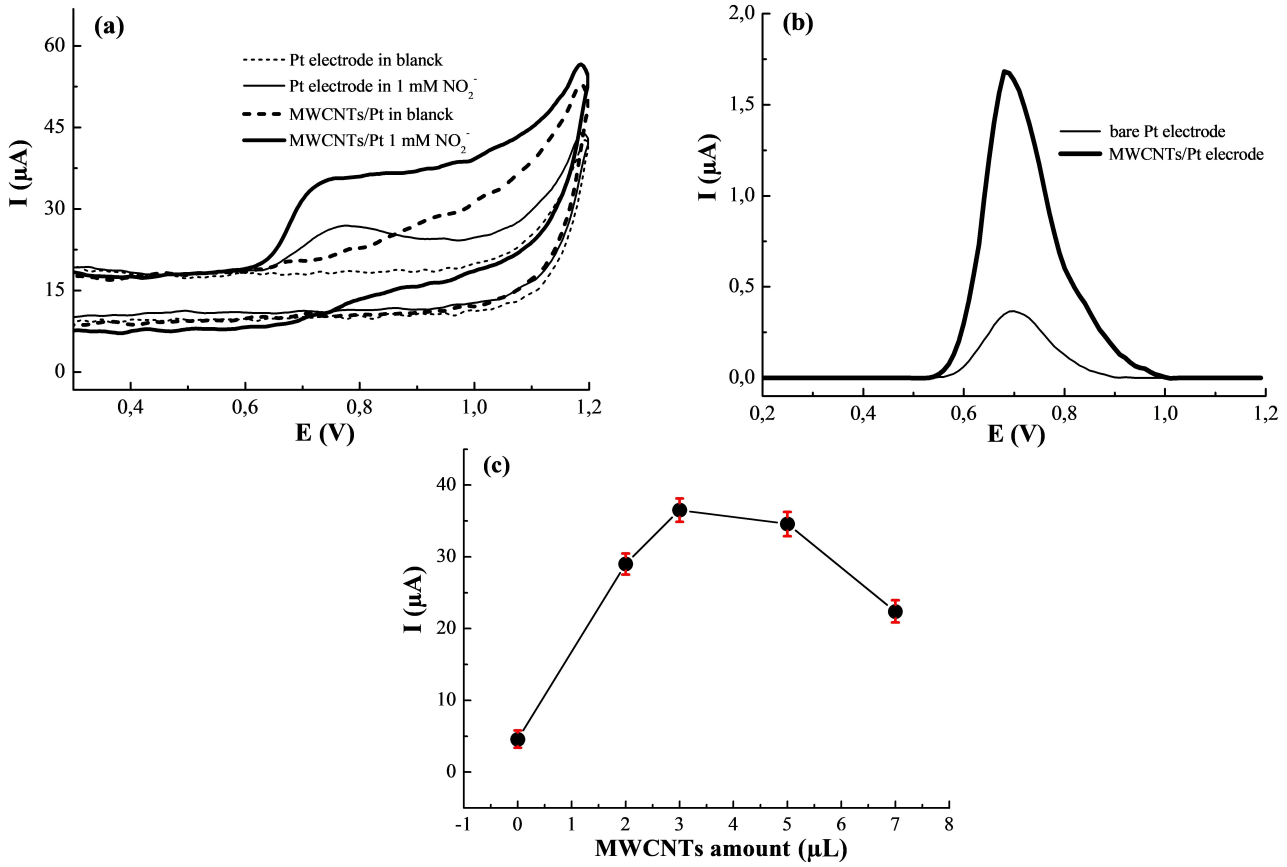

Figure 1. Electrochemical behavior. (a) Cyclic voltammograms of the bare Pt and MWCNTs/Pt in the absence and presence of 1.0 mM NO_2^- in 0.1 M PBS at pH 7.0; (b) SWV response of the bare Pt and MWCNTs/Pt with 1.0 mM NO_2^- in 0.1 M PBS at pH 7.0; (c) effect of the MWCNTs amount on the current response of 1 mM NO_2^-. MWCNTs: multi-walled carbon nanotubes

In addition, when the obtained SWV results were compared (Figure 1b), the MWCNTs/Pt shows a higher response current, which presents an increase of more than four times in the voltammetric response

compared to the bare Pt electrode. This indicates that the MWCNTs/Pt improves the electrochemical reaction of NO_2^- compared with bare Pt electrode. The enhanced signal is probably due to the facile electron transfer with an improved rate and larger active surface area of the modified electrode.

The effect of MWCNT amounts on the peak current response of 1 mM NO_2^- was examined (Figure 1c). In this regard, different volumes of the suspension were cast on the bare Pt. The best response of NO_2^- was obtained when a 3 µL drop was used. Therefore, the amount of MWCNTs chosen for the preparation of the sensor was fixed at 3 µL.

Electrochemical characterization of MWCNTs/Pt

The cyclic voltammograms of bare Pt and MWCNTs/Pt electrodes were carried out in 1.0 mM $[Fe(CN)_6]^{3-/4-}$ containing 0.1 M KCl at a scan rate of 50 mVs^{-1} (Figure 2a). A pair of redox peaks were observed at both unmodified and modified electrodes. The peak current at the modified electrode increases dramatically compared with that observed at the bare Pt electrode, suggesting that MWCNTs/Pt exhibits faster electron transfer kinetics compared with the bare Pt electrode. Using the Randles-Sevcik relation [20]:

$$I_p = (2.69 \times 10^5) \times n^{\frac{3}{2}} A D_o^{\frac{1}{2}} v^{\frac{1}{2}} C_o \quad (1)$$

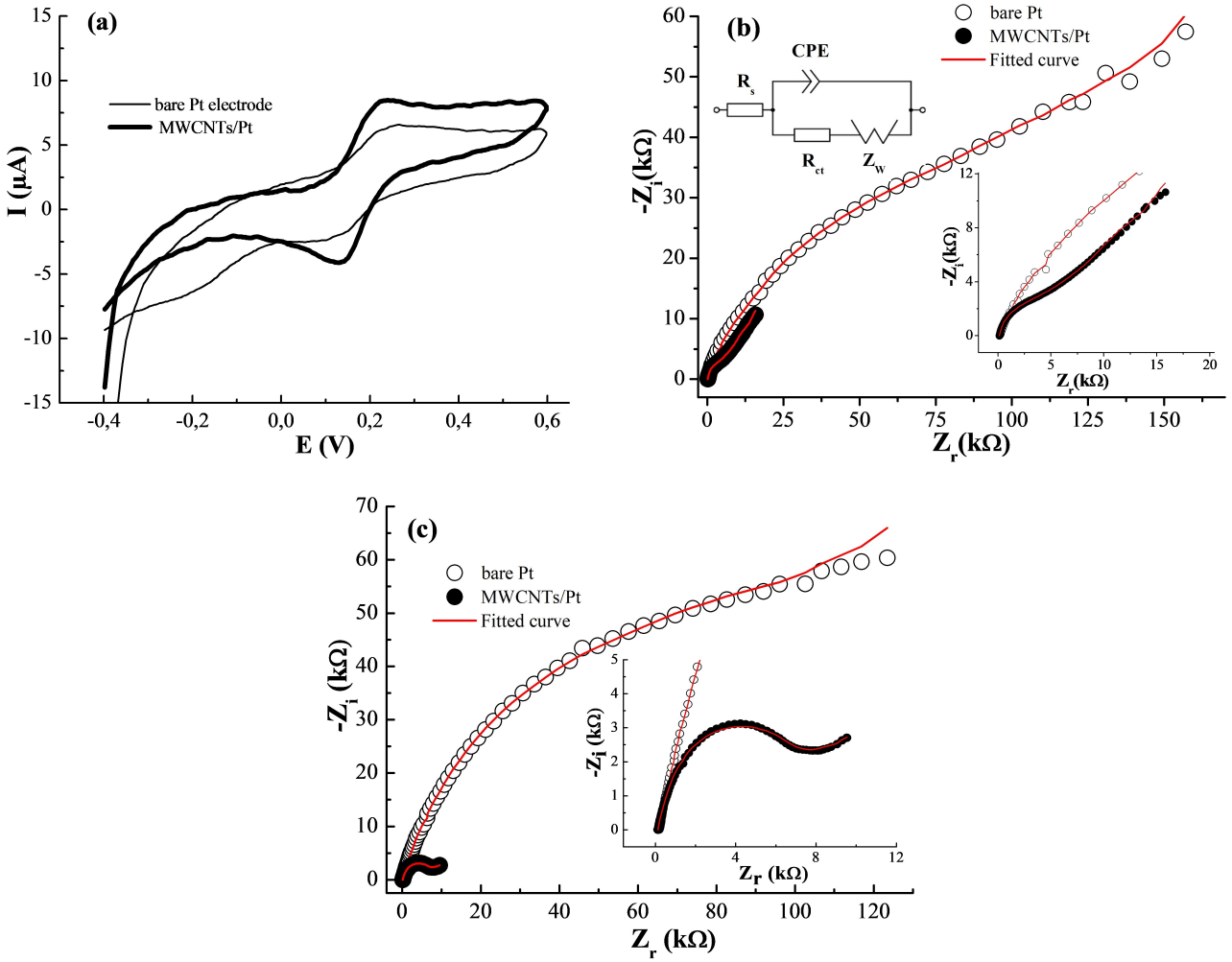

Figure 2. Electrochemical characterization. (a) Cyclic voltammograms; (b) Nyquist plots of bare Pt and MWCNTs/Pt in 0.1 M KCl containing 1.0 mM $K_3[Fe(CN)_6]$; (c) Nyquist plots of bare Pt and MWCNTs/Pt in 0.1 M PBS (pH = 7.0) containing 1 mM NO_2^-. Inset (b): Randles electrical circuit of the redox system. CPE: constant phase element

Where n, C_o, A, v, and D_o are the number of electrons involved, the substrate concentration (1.0 mM), the active surface area, the scan rate, and the diffusion coefficient of ferrocenium/ferrocene (7.6×10^{-6} cm/s [21]) respectively. The surface area of MWCNTs/Pt and bare Pt electrode are respectively 0.042 and

0.035 cm^2. The results clearly show that the electrode modified with MWCNTs film has a larger active surface area, which results in higher sensitivity.

EIS analysis of the bare Pt and MWCNTs/Pt was performed to explain the electron transfer changes between the modified electrode and the solution interface in the presence of 10 mM $[Fe(CN)_6]^{3-/4-}$ containing 0.1 M KCl. In the EIS plots (Figure 2b), the high-frequency region of the impedance real part presents the solution resistance (R_s). The semicircular part at high frequency illustrates the electron transfer resistance (R_{ct}) while the straight line at the low-frequency ranges is ascribed to the diffusion of $K_3Fe(CN)_6/K_4Fe(CN)_6$ as the redox probe (Warburg impedance, W) [22–25]. Moreover, a constant phase element (CPE) is introduced to take into account the topological imperfections of the materials caused by the surface roughness of the electrode. The impedance (Z_{CPE}) is characterized by a slight deviation from pure capacitive behavior and is then given by [22, 23]:

$$Z(CPE) = \frac{1}{Q(j\omega)^{\alpha}} \quad (2)$$

Where $j = (-1)^{1/2}$, $\omega = 2\pi f$ being f the frequency of the applied ac potential, $Q = C\omega_{max}^{1-\alpha}$ and α is fractional and its experimental value is between 0.5 (for an ideally porous electrode) and 1 (for a perfect smooth electrode). The EIS parameters were fitted by Zview using the Randles electrical circuit (Figure 2b, insert). The results of the simulations are reported in Figure 2b (curves in red) which show a very good correspondence with the experimental data. The values of each component are shown in Table 1. As seen, the bare Pt electrode has exhibited a large semicircle with a high R_{ct} value, while the diameter of the semicircle of the MWCNTs/Pt electrode is much smaller with a low R_{ct} value compared to the bare electrode. By contrast, the values of Q are opposed to the R_{ct} values, which indicates that the electronic transport and mass transport resistance of MWCNTs/Pt electrodes is much smaller than those of bare Pt electrodes. Moreover, the W value of the redox probe at the bare Pt electrode is 597.8 kΩ and is decreased to 41.37 kΩ at the modified electrode, which proves that the MWCNTs film may increase the diffusion rate of the electroactive species towards the electrode surface.

Table 1. EIS parameters obtained from the equivalent circuit proposed in Figure 2b

Electrode	R_s, kΩ	R_{ct}, kΩ	Q, $\mu Fs^{\alpha-1}$	W, kΩ	α
Bare Pt	166	50.70	2.55	597.8	0.70
MWCNTs/Pt	135	4.27	14.20	41.37	0.86

MWCNTs: multi-walled carbon nanotubes

EIS was also used to investigate the charge transfer property of different electrodes in 0.1 M PBS (pH = 7.0) aqueous solution having 1 mM NO_2^- (Figure 2c). By fitting the Randles equivalent electrical circuits, the R_{ct} caused by the faradaic reactions at the MWCNTs/electrolyte interface has a smaller semicircle diameter of 8.3 kΩ compared to 141.8 kΩ recorded for the bare Pt electrode. This feature suggests that MWCNTs improve the surface conductivity and hence the electron transfer kinetics of the analyte. Therefore, the MWCNTs/Pt-modified electrode was considered to be used in the application of nitrite electrochemical determination.

Scan rate study

The influence of scan rate on nitrite oxidation at MWCNTs/Pt was examined to investigate the kinetic mechanism of nitrite oxidation behavior. Figure 3a shows a cyclic voltammogram of the NO_2^- at various sweeping rates (5–300 mVs^{-1}) in 0.1 M PBS solution at pH 7.0 using MWCNTs/Pt. The current responses are increased linearly with the square root of the scan rates ($v^{1/2}$) (Figure 3b). This supports that the oxidation of NO_2^- is governed by the diffusion of the analyte at the MWCNTs/Pt electrode.

To support these results, the dependence of log I_p on log v was investigated (Figure 3c). Normally, the slope is close to 0.5 for a diffusion-controlled and 1.0 for an adsorption-controlled process [26]. The dependence of log I_p with log v for the nitrite oxidation peak gives a slope of 0.47 with a correlation

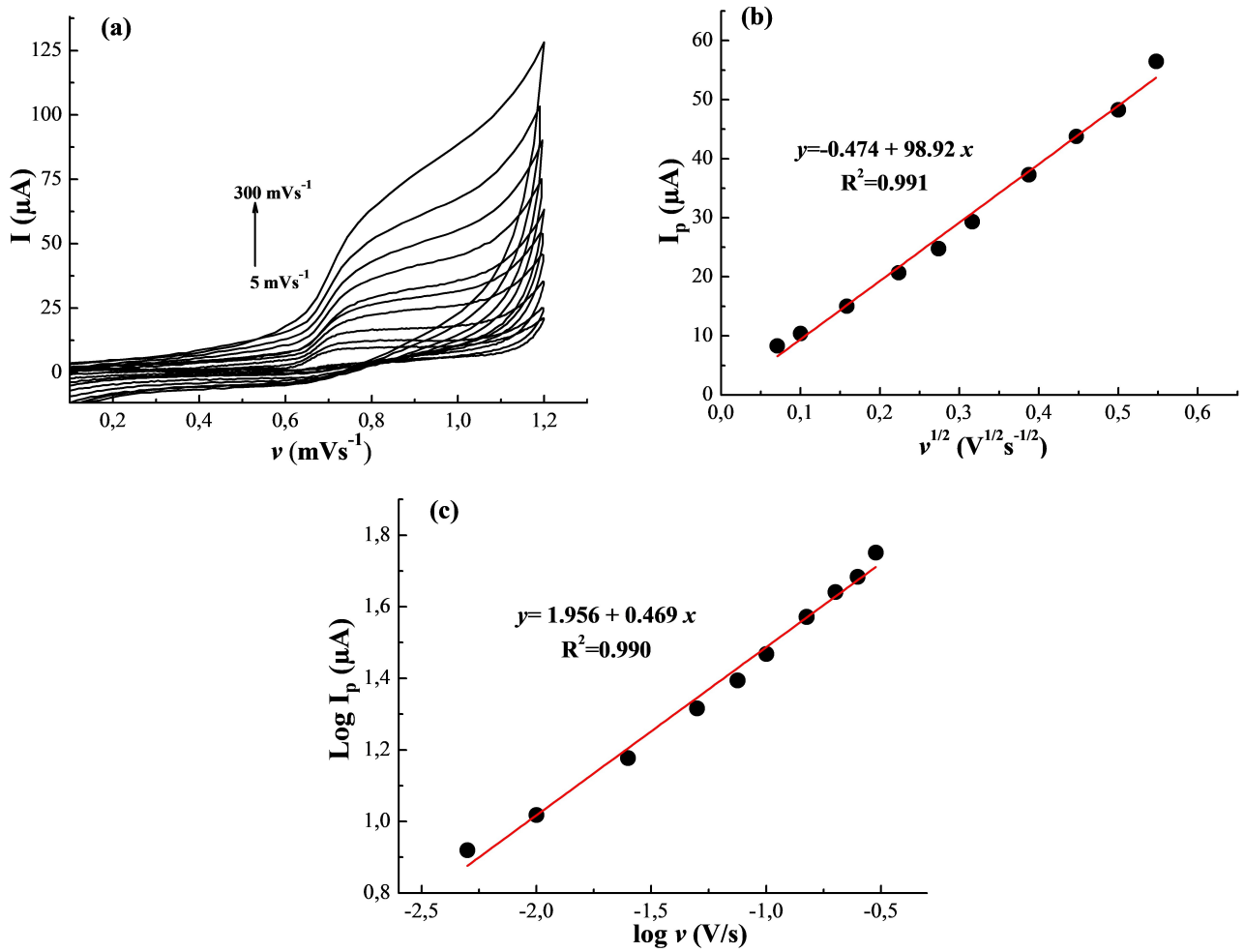

Figure 3. Kinetic of electrode process. (a) Cyclic voltammograms of the MWCNTs/Pt in 0.1 M PBS (pH 7.0) containing 1.0 mM NO_2^- at different scan rates (5–300 mVs^{-1}); (b) linear relationship between anodic peak current and square root of scan rate; (c) linear relationship between log I_p and logarithmic scan rate

coefficient close to unity (0.99), corroborating a diffusion-controlled electron transfer process of NO_2^- on the proposed sensor.

Therefore, the number of electrons (n) involved in the reaction can be extracted from the relation [27]:

$$\Delta E = E_p - E_{\frac{p}{2}} = \frac{47.7}{\alpha n} (\text{mV}) \quad (3)$$

Where E_p is the peak potential, and $E_{p/2}$ is the half-peak potential. Thus, αn was found to be 1.0. The coefficient α is equal to 0.5 for an irreversible system. The number of exchanged electrons in the NO_2^- oxidation is equal to 2.0, involving two electrons in the NO_2^- oxidation to NO_3^- in agreement with previous reports on nitrite oxidation [28–32]. Hence, the following reaction is suggested:

$$NO_2^- + H_2O \rightarrow NO_3^- + 2H^+ + 2e^- \quad (4)$$

Effects of pH

Figure 4 depicts the current responses obtained at different pH values for the electro-oxidation of 1 mM NO_2^- on MWCNTs/Pt. As can be seen, the current response augments from pH 5.0 to 7.0, reaching a maximal pH of 7.0 and then decreases up to pH 9.0. Such results indicate that the pH domain is small in both acid and alkaline solutions, while the neutral pH is a suitable medium for the electro-catalytic oxidation of NO_2^- [32]. Hence, subsequent detection of NO_2^- was performed in PBS solution buffered at pH 7.0.

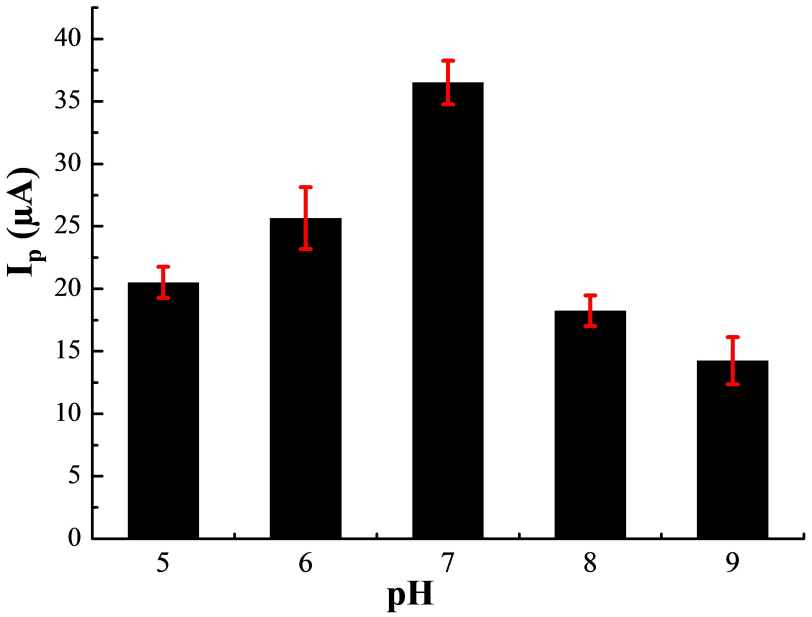

Figure 4. Voltammetric responses of the modified electrode at different pHs in 0.1 M PBS containing 1.0 mM NO_2^-

Chronoamperometric study

The electrocatalytic oxidation of NO_2^- on MWCNTs/Pt was also studied by ChAm in 0.1 M PBS (pH 7.0) having 10 μM NO_2^- at an applied potential of 0.7 V (Figure 5). Plotting the net current against $t^{-1/2}$ exhibits a linear relation (Figure 5, insert a), with a dominant diffusion-controlled process. By using the slope of this plot, the diffusion coefficient (D) of NO_2^- can be extracted from the Cottrell relation [33]:

$$I = nFAD^{\frac{1}{2}}C_0\pi^{-\frac{1}{2}}t^{-\frac{1}{2}} \quad (5)$$

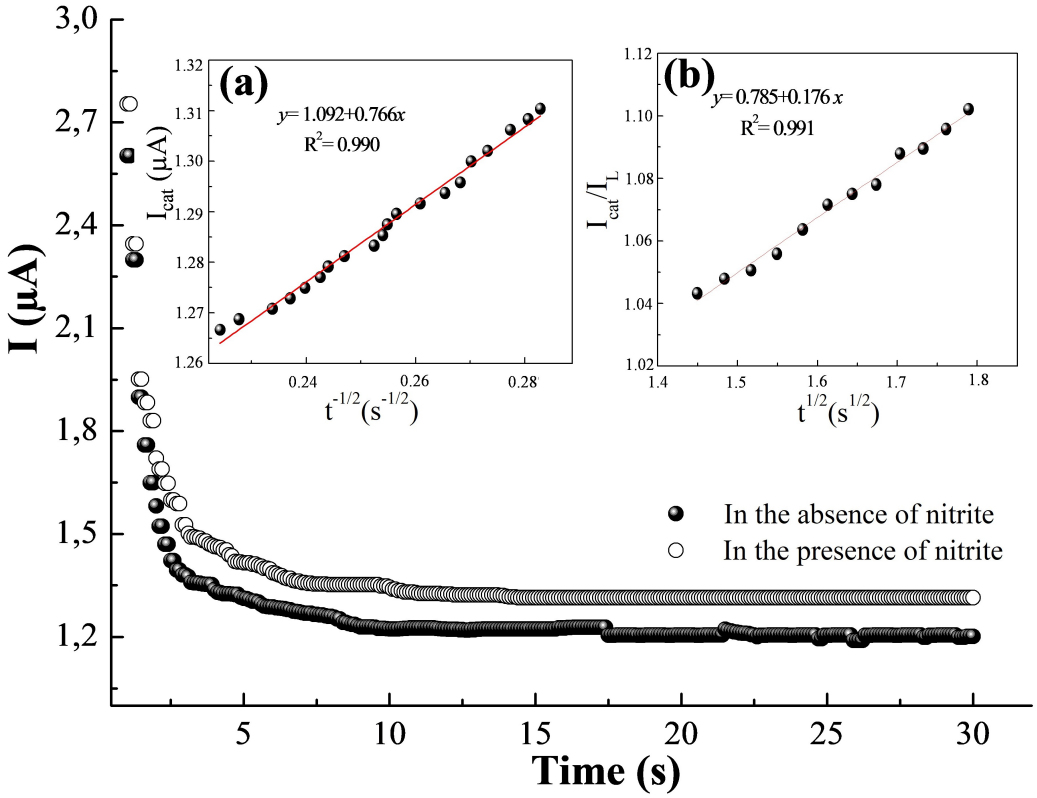

Figure 5. Chronoamperograms were recorded for MWCNTs/Pt in 0.1 M PBS (pH 7.0) in the absence and presence of 10 μM NO_2^-. Insert (a): dependence of I_{cat} vs. $t^{-1/2}$; insert (b): dependence of I_{cat}/I_L vs. $t^{1/2}$

Where C_o is the bulk concentration. The diffusion coefficient of NO_2^- is found to be 1.44×10^{-5} cm^2/s which is close to formerly reported values [34, 35]. This technique was also used to estimate the catalytic rate constant (k) for the interface reaction between the nitrite and the modified electrode according to equation [36]:

$$I_{cat}/I_L = \gamma^{\frac{1}{2}}[\pi^{\frac{1}{2}}\mathrm{erf}(\gamma^{\frac{1}{2}}) + \exp(-\gamma)/\gamma^{\frac{1}{2}}] \quad (6)$$

Where I_{cat} and I_L are the amperometric currents of the MWCNTs/Pt with and without NO_2^- respectively, γ (= kC_0t) is the argument of the error function, and t is the elapsed time (s). When $\gamma > 1.5$, erf ($\gamma^{1/2}$) is very close to 1 and the simplified equation becomes:

$$I_{cat}/I_L = \gamma^{\frac{1}{2}}\pi^{\frac{1}{2}} = \pi^{\frac{1}{2}}(kC_0t)^{\frac{1}{2}} \quad (7)$$

From the slope of the (I_{cat}/I_L) versus $t^{1/2}$ plot (Figure 5, insert b), the value of k was obtained as 1.43×10^4 $M^{-1}s^{-1}$.

SWV detection of nitrite at MWCNTs/Pt

SWV is a pulse-sensitive method that could attenuate the background noise, allowing a higher sensitivity than the CV for low analyte concentrations [37]. SWV was performed in 0.1 M PBS (pH = 7.0) using a pulse duration time of 0.05 s, pulse amplitude of 25 mV, frequency of 50 Hz, a scan rate of 10 mVs^{-1}, and a step potential of 10 mV. A well-defined nitrite oxidation peak is observed at 0.67 V as shown in Figure 6a. The peak current increases linearly with increasing the NO_2^- amount in the concentration ranges from 1.0 to 1,000 µM (Figure 6b). The LOD of the fabricated sensor is found as 0.1 µM taking LOD = 3 s/m, where s is the standard deviation of the current of low NO_2^- concentration and m is the slope of the calibration graph (n = 5) [38]. The LOD is well below the maximum allowable limit for NO_2^- in potable water (43.48 µM) according to the WHO directives [3]. The relative standard deviations (RSD) were evaluated at 1.5% for five separate voltammograms of 50 µM NO_2^-. Therefore, our sensor is better suited to assess NO_2^- concentrations in real water. The analytical parameters of the elaborated electrode are listed in Table 2. The electrocatalytic performance of MWNCNTs/Pt for the oxidation of NO_2^- was superior or comparable to previously reported results as displayed in Table 3. The improved sensing performance of MWCNTs/Pt can be attributed to their good conductivity and large surface area. These results for the MWCNTs/Pt system reveal a good analytical performance in terms of simplicity and efficiency for the detection of this analyte.

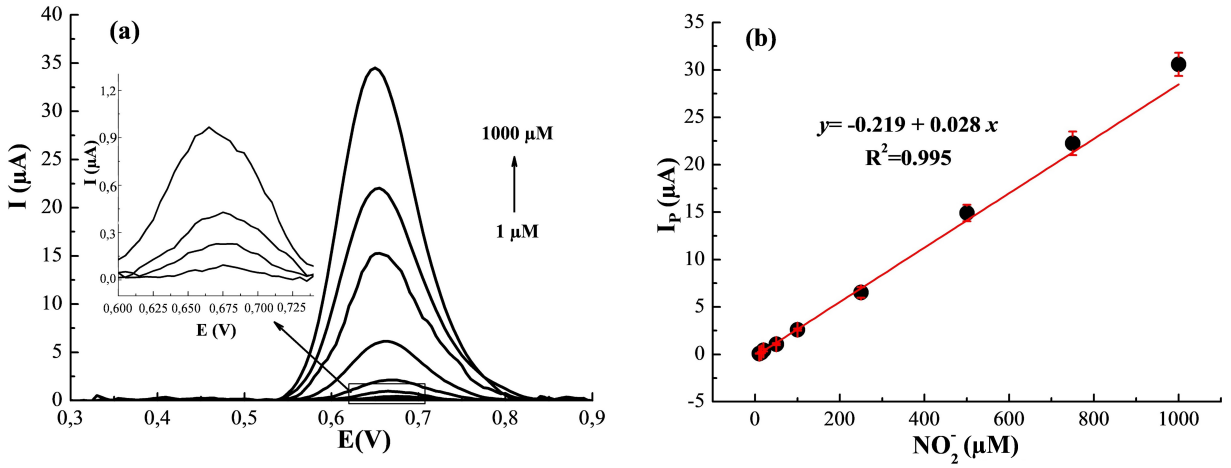

Figure 6. Electroanalytical performance. (a) SWV with varying concentrations (1–1,000 µM) of NO_2^- using the MWCNTs/Pt in 0.1 M PBS at pH 7.0; (b) analytical curve of I_p vs. NO_2^- concentration

Table 2. Analytical parameters of the calibration curve of nitrite on MWCNTs/Pt using the SWV method

Analytical parameters	0.1 M PBS (pH = 7)
Peak potential, V	0.67
Linearity range, µM	1.0–1,000

Table 2. Analytical parameters of the calibration curve of nitrite on MWCNTs/Pt using the SWV method (*continued*)

Analytical parameters	0.1 M PBS (pH = 7)
Slope, μA/μM	0.028
Intercept, μA	–0.219
Correlation coefficient	0.995
SE of slope	0.0006
SE of intercept	0.001
LOD, μM	0.10
LOQ, μM	0.35
Within-day of peak current (RSD %)[a]	0.32
Within-day of peak potential (RSD %)[a]	0.02
Between-day of peak current (RSD %)[a]	1.89
Between-day of peak potential (RSD %)[a]	0.10

[a] Obtained from five measurements. PBS: phosphate-buffered solution; SE: standard error; LOD: limit of detection; RSD: relative standard deviation

Table 3. The performance of the different modified electrodes for the detection of NO_2^-

Electrode materials	Medium	Potential (V)	LR (μM)	LOD (μM)	Ref.
Ag-HNT MoS_2/GCE	0.1 M PBS (pH = 4)	0.8 V (Ag/AgCl)	2–425	0.7	[9]
PEDOT-AuNPs/GCE	0.1 M PBS (pH = 5)	0.78 V (SCE)	3–300	0.1	[10]
rGO-MoS_2/GCE	0.1 M PBS (pH = 7)	0.8 V (Ag/AgCl)	0.2–4,800	0.17	[11]
Cu/Ag/MWCNTs/GCE	0.1 M PBS (pH = 7)	0.85 V (SCE)	1–1,000	0.2	[12]
nHAP-PEDOT/GCE	0.2 M PBS (pH = 8)	0.78 V (SCE)	0.25–1.05	0.083	[30]
Fe_2O_3-MoS_2/GCE	0.1 M PBS (pH = 4)	1.0 V (SCE)	2–6,730	1.0	[31]
CG-Ppy-CS/GCE	0.1 M AcHAC (pH = 4)	0.87 V (Ag/AgCl)	0.2–1,000	0.02	[32]
Poly (4-AB/OT)/CPE	0.1 M PBS (pH = 5)	0.95 V (Ag/AgCl)	6–600	3.5	[33]
a-Fe_2O_3/CNTs/GC	0.1 M PBS (pH = 7)	0.95 V (Ag/AgCl)	0.5–4,000	0.15	[39]
MWCNTs/Pt	0.1 M PBS (pH = 7)	0.70 V (SCE)	1–1,000	0.1	This work

GCE: glassy carbon electrode; PBS: phosphate-buffered solution; CPE: carbon-paste electrode; AuNPs: gold nanoparticles; SCE: saturated calomel electrode; Poly (4-AB/OT): poly(4-aminobenzoic acid/o-toluidine); Ppy: polypyrrole; CG: carboxyl graphene; nHAP: nanosized hydroxyapatite; MWCNTs: multi-walled carbon nanotubes; LR: linear range; LOD: limit of detection; HNT: halloysite nanotube; GC: galssy carbon; PEDOT: poly(3,4-ethylenedioxythiophene); rGO: reduced graphene oxide; CNTs: carbon nanotubes; CS: chitosan; AcHAC: acetic acid-sodium acetate

Reproducibility, stability, and interference analyses of sensor

To test the stability of the MWCNTs/Pt electrode, the current responses of 50 μM NO_2^- were followed for 5 consecutive days. The oxidation current of NO_2^- remains practically unchanged with an RSD not exceeding 1.5% for five successive tests, showing clearly that the prepared electrode possesses good stability. Additionally, the reproducibility of the proposed sensor was tested with five different fabricated electrodes in 50 μM NO_2^-, and the RSD of the current signal was obtained as 2.04%, suggesting the good reproducibility of this electrochemical sensor.

In order to investigate the anti-interference property of the modified electrode, the effects of common interfering minerals and organic substances on the response sensor were examined. The electrode response to a 50 μM tested solution of NO_2^- in 0.1 M PBS (pH 7.0) is 1.26 μA. After adding 100-fold excess amounts of Na^+, Cl^-, K^+, Zn^{2+}, Ba^{2+}, Mn^{2+}, glucose, and ascorbic acid to the tested nitrite solution, no interference effect for the nitrite determination was observed (Table 4). The relative error values for the response were smaller than ± 5%, suggesting that the MWCNTs/Pt sensing electrode has good selectivity toward NO_2^- detection.

Table 4. The effects of interfering substances on NO_2^- sensor

Interfering substances	Current (μA)	Relative error (%)
Na^+	1.21	–3.96
Cl^-	1.25	–0.78

Table 4. The effects of interfering substances on NO_2^- sensor (*continued*)

Interfering substances	Current (μA)	Relative error (%)
K^+	1.24	–1.58
Ba^{2+}	1.19	–3.45
Mn^{2+}	1.31	+3.96
Zn^{2+}	1.32	+4.76
Ascorbic acid	1.27	+0.79
Glucose	1.21	–3.90

Analysis of nitrite in real samples

To verify the practical applicability of the proposed sensor, NO_2^- was analyzed on MWCNTs/Pt. Known concentrations of NO_2^- were added to both mineral and source waters. The recovery study was realized thanks to the standard addition technique and the method can be applied for the NO_2^- detection in real effluents (Table 5).

Table 5. Recovery study with the proposed method

Samples	Added (μM)	Found (μM)	Recovery (%)	RSD % (*n* = 5)	Bias % (*n* = 5)
Mineral water	50	49.58 ± 1.33	99.16	2.68	2.00
Source water	50	51.04 ± 0.89	102.08	1.74	5.30

RSD: relative standard deviation

Discussion

In summary, a novel sensor for the determination of nitrite was constructed using MWCNTs coated Pt electrode. The MWCNTs/Pt exhibited good electrocatalytic activity towards the oxidation of nitrite. Compared with previous reports for nitrite response, the method for nitrite determination displayed a good LOD of 0.1 μM. The main reason was ascribed to the large surface area and good conductivity of the modified electrode, which improves the electrode reaction kinetic towards NO_2^-. The results of this study indicate that the developed sensor has great potential for applications in the analysis of real samples including source water and mineral water.

Abbreviations

ChAm: chronoamperometry

CV: cyclic voltammetry

DMF: *N*,*N*-dimethylformamide

EIS: electrochemical impedance spectroscopy

LOD: limit of detection

MWCNTs: multi-walled carbon nanotubes

PBS: phosphate-buffered solution

RSD: relative standard deviation

SCE: saturated calomel electrode

SWV: square wave voltammetry

Declarations

Author contributions

MD: Conceptualization, Writing—original draft, Writing—review & editing, Investigation, Supervision. NKB: Investigation, Validation, Writing—review & editing. BS: Investigation. MT and SAO: Writing—review & editing. All authors read and approved the submitted version.

Conflicts of interest

The authors declare have no conflict of interest in financial, personal, or other relationships with other people, laboratories, or organizations.

Ethical approval

Not applicable.

Consent to participate

Not applicable.

Consent to publication

Not applicable.

Availability of data and materials

The raw data supporting the conclusions of this manuscript will be made available by the authors, without undue reservation, to any qualified researcher.

Funding

Not applicable.

References

1. Xue Z, Fu X, Rao H, Zhou X, Liu X, Lu X. A new electron transfer mediator actuated non-enzymatic nitrite sensor based on the voltammetry synthetic composites of 1-(2-pyridylazo)-2-naphthol nanostructures coated electrochemical reduced graphene oxide nanosheets. Electrochim Acta. 2018; 260:623–9. [DOI]
2. Ahmad R, Mahmoudi T, Ahn M, Yoo J, Hahn Y. Fabrication of sensitive non-enzymatic nitrite sensor using silver-reduced graphene oxide nanocomposite. J Colloid Interface Sci. 2018;516:67–75. [DOI] [PubMed]
3. Mounesh, Reddy KRV. Sensitive and reliable electrochemical detection of nitrite and H_2O_2 embellish-CoPc coupled with appliance of composite MWCNTs. Anal Chim Acta. 2020;1108:98–107. [DOI] [PubMed]
4. Filik H, Giray D, Ceylan B, Apak R. A novel fiber optic spectrophotometric determination of nitrite using Safranin O and cloud point extraction. Talanta. 2011;85:1818–24. [DOI] [PubMed]
5. Shah I, Petroczi A, James RA, Naughton DP. Determination of Nitrate and Nitrite Content of Dietary Supplements Using Ion Chromatography. J Anal Bioanal Tech. 2013;S12:003. [DOI]
6. Tian YS, Li XH, Zhang DF, Lu L, Xu YG, An CW. A Novel Method for the Polarographic Determination of Trace Nitrite in Water. Russ J Electrochem. 2022;58:32–42. [DOI]
7. Farsang R, Kovacs Z, Jarvas G, Guttman A. Ultrahigh-Sensitivity Capillary Electrophoresis Analysis of Trace Amounts of Nitrate and Nitrite in Environmental Water Samples. Separations. 2022;9:333. [DOI]
8. Hallaj R, Salimi A, Kavosi B, Mansouri G. Highly sensitive and ultra-selective amperometric nitrite sensor using cyclometalated Rh(III)-complex/CNTs modified glassy carbon electrode integrated with flow injection analysis. Sens Actuators B: Chem. 2016;233:107–19. [DOI]
9. Ghanei-Motlagh M, Taher MA. A novel electrochemical sensor based on silver/halloysite nanotube/molybdenum disulfide nanocomposite for efficient nitrite sensing. Biosens Bioelectron. 2018;109: 279–85. [DOI] [PubMed]

10. Zhang D, Fang Y, Miao Z, Ma M, Du X, Takahashi S, et al. Direct electrodeposion of reduced graphene oxide and dendritic copper nanoclusters on glassy carbon electrode for electrochemical detection of nitrite. Electrochim Acta. 2013;107:656–63. [DOI]
11. Hu J, Zhang J, Zhao Z, Liu J, Shi J, Li G, et al. Synthesis and electrochemical properties of rGO-MoS_2 heterostructures for highly sensitive nitrite detection. Ionics. 2018;24:577–87. [DOI]
12. Zhang Y, Nie J, Wei H, Xu H, Wang Q, Cong Y, et al. Electrochemical detection of nitrite ions using Ag/Cu/MWNT nanoclusters electrodeposited on a glassy carbon electrode. Sens Actuators B: Chem. 2018; 258:1107–16. [DOI]
13. Liu L, Cui H, An H, Zhai J, Pan Y. Electrochemical detection of aqueous nitrite based on poly(aniline-*co*-*o*-aminophenol)-modified glassy carbon electrode. Ionics. 2017;23:1517–23. [DOI]
14. Rajalakshmi K, John SA. Highly sensitive determination of nitrite using FMWCNTs-conducting polymer composite modified electrode. Sens Actuators B: Chem. 2015;215:119–24. [DOI]
15. Zhang S, Li B, Sheng Q, Zheng J. Electrochemical sensor for sensitive determination of nitrite based on the CuS–MWCNT nanocomposites. J Electroanal Chem. 2016;769:118–23. [DOI]
16. Cheraghi S, Taher MA, Fazelirad H. Voltammetric determination of silver with a new multi-walled carbon nanotube modified paste electrode. Russ J Electrochem. 2015;51:271–7. [DOI]
17. Ghalkhani M, Shahrokhian S, Ghorbani-Bidkorbeh F. Voltammetric studies of sumatriptan on the surface of pyrolytic graphite electrode modified with multi-walled carbon nanotubes decorated with silver nanoparticles. Talanta. 2009;80:31–8. [DOI] [PubMed]
18. Frueh J, Nakashima N, He Q, Möhwald H. Effect of linear elongation on carbon nanotube and polyelectrolyte structures in PDMS-supported nanocomposite LbL films. J Phys Chem B. 2012;116: 12257–62. [DOI] [PubMed]
19. Decher G, Hong JD. Buildup of ultrathin multilayer films by a self-assembly process, 1 consecutive adsorption of anionic and cationic bipolar amphiphiles on charged surfaces. Makromol Chem. Macromol Symp. 1991;46:321–7. [DOI]
20. Trojanowicz M. Analytical applications of carbon nanotubes: a review. TrAC Trends Anal Chem. 2006; 25:480–9. [DOI]
21. Bard AJ, Faulkner LR. Electrochemical Methods: Fundamentals and Applications. 2nd ed. New York: Wiley; 2001. p. 231.
22. Zhao YD, Zhang WD, Luo QM, Li SFY. The oxidation and reduction behavior of nitrite at carbon nanotube powder microelectrodes. Microchem J. 2003;75:189–98. [DOI]
23. Tehrani RMA, Ghadimi H, Ab Ghani S. Electrochemical studies of two diphenols isomers at graphene nanosheet–poly(4-vinyl pyridine) composite modified electrode. Sens Actuators B: Chem. 2013;177: 612–9. [DOI]
24. Qu Q, Chen Z, Sun GT, Qiu L, Zhu MQ. $CoFe_2O_4$ nanoparticles as a bifunctional agent on activated porous carbon for battery-type asymmetrical supercapacitor. Chem Synth. 2024;4:26. [DOI]
25. Srinivas K, Yu H, Chen Z, Chen A, Zhu M, Chen Y, et al. Densely accessible Fe/Co–N_x dual-atom site coupled core–shell Co_3Fe_7@C as an efficient bifunctional oxygen electrocatalyst for rechargeable zinc–air batteries. J Mater Chem A. 2024;12:16863–76. [DOI]
26. Dong YP, Zhou Y, Ding Y, Chu XF, Wang CM. Sensitive detection of Pb(ii) at gold nanoparticle/polyaniline/graphene modified electrode using differential pulse anodic stripping voltammetry. Anal Methods. 2014;6:9367–74. [DOI]
27. Huang Y, Shih H, Mansfeld F. Concerning the use of constant phase elements (CPEs) in the analysis of impedance data. Mater Corros. 2010;61:302–5. [DOI]
28. Hammam E. Determination of nitrofurantoin drug in pharmaceutical formulation and biological fluids by square-wave cathodic adsorptive stripping voltammetry. J Pharm Biomed Anal. 2002;30:651–9. [DOI] [PubMed]

29. Ensafi AA, Karimi-Maleh H. Modified multiwall carbon nanotubes paste electrode as a sensor for simultaneous determination of 6-thioguanine and folic acid using ferrocenedicarboxylic acid as a mediator. J Electronal Chem. 2010;640:75–83. [DOI]
30. Wang G, Han R, Feng X, Li Y, Lin J, Luo X. A glassy carbon electrode modified with poly(3,4-ethylenedioxythiophene) doped with nano-sized hydroxyapatite for amperometric determination of nitrite. Microchim Acta. 2017;184:1721–7. [DOI]
31. Wang H, Chen P, Wen F, Zhu Y, Zhang Y. Flower-like Fe_2O_3@MoS_2 nanocomposite decorated glassy carbon electrode for the determination of nitrite. Sens Actuators B: Chem. 2015;220:749–54. [DOI]
32. Xiao Q, Feng M, Liu Y, Lu S, He Y, Huang S. The graphene/polypyrrole/chitosan-modified glassy carbon electrode for electrochemical nitrite detection. Ionics. 2018;24:845–59. [DOI]
33. Norouzi B, Rajabi M. Fabrication of poly(4-aminobenzoic acid/*o*-toluidine) modified carbon paste electrode and its electrocatalytic property to the oxidation of nitrite. J Anal Chem. 2017;72:897–903. [DOI]
34. Jiang LY, Wang RX, Li XM, Jiang LP, Lu GH. Electrochemical oxidation behavior of nitrite on a chitosan-carboxylated multiwall carbon nanotube modified electrode. Electrochem Commun. 2005;7:597–601. [DOI]
35. Etesami M, Chandran Nurul SNMS, Hussin MH, Ripin A, Adnan R, Sujari ANA, et al. Electrooxidation of Nitrite Ions on Gold/Polyaniline/Carbon Paste Electrode. Int J Electrochem Sci. 2016;11:8332–45. [DOI]
36. Jeena SE, Gnanaprakasam P, Dakshinamurthy A, Selvaraju T. Tuning the direct growth of Ag_{seeds} into bimetallic Ag@Cu nanorods on surface functionalized electrochemically reduced graphene oxide: enhanced nitrite detection. RSC Adv. 2015;5:48236–45. [DOI]
37. Yadav SK, Agrawal B, Goyal RN. AuNPs-poly-DAN modified pyrolytic graphite sensor for the determination of Cefpodoxime Proxetil in biological fluids. Talanta. 2013;108:30–7. [DOI] [PubMed]
38. Aboul-Enein, H.Y. Sibel A. Ozkan: Electroanalytical Methods in Pharmaceutical Analysis and Their Validation. Chromatographia 75, 811 (2012) [DOI]
39. Zhe T, Li R, Wang Q, Shi D, Li F, Liu Y, et al. *In situ* preparation of FeSe nanorods-functionalized carbon cloth for efficient and stable electrochemical detection of nitrite. Sens Actuators B: Chem. 2020;321: 128452. [DOI]